Egypt. J. Chem. **Vol. 64,** No. 4 pp. 1653 - 1664 (2021)

Egyptian Journal of Chemistry

http://ejchem.journals.ekb.eg/

High-Performance Rheology Modifiers And Fluid Loss Of Starch-Bentonite System Based Mud Fluids: Experimental And Optimization Study

Hany E. Ahmed[a], Mohamed A. Betiha[a], Mona El-Dardir[a], Modather F. Hussein[b,c] Nabel A. Negm[a#]

[a] *Egyptian Petroleum Research Institute, Nasr City, Cairo 11727, Egypt*

[b] *Chemistry Department, College of Science, Jouf University, P. O. Box 2014, Sakaka, Aljouf, Saudi Arabia*

[c] *Chemistry Department, Faculty of Science, Al-Azhar University, Assiut 71524, Egypt*

Abstract

The capability of drilling fluid to endure high temperatures is an important characteristic of drilling fluids. Natural polymers are commonly used as additives for drilling fluids to improve their rheological properties. Starch is one of them, that is extensively used in the drilling due to economics. However, the thermal stability of water-based mud included starch is low. Herein, diethanolamine is used to enhance the rheological and filtration loss properties of the water-based fluids (WBF) through chemical modification of Lewis acid sites in bentonite framework and the formation of a cross-linked hydrogen bond with the starch compound. The effect of starch as an additive to WBF was studied at 0.56% and 0.94% in the bentonite-based fluid. The revealed data indicated an apparent improvement had been achieved after the addition of starch (0.94%). The effect of diethanolamine (DEA) on the rheological properties of starch-bentonite system, DEA was used as an additive at three ratios of 0.19%, 0.37%, and 0.75, at 300 °F, 325 °F, 350 °F, and 375 °F. The obtained data indicated that both rheological and filtration loss properties were enhanced, eventually at elevated temperature of 350 °F. The interaction in bentonite-starch, bentonite-DEA, and bentonite-starch-DEA WBF was studied using FTIR, XRD, and Raman spectroscopy. The results indicated the formation of hydrogen bonds between all components, which increases the basal displacing between bentonite layers. That interaction leads to the enhancement of the rheological and filtration loss properties of the drilling fluid. The response surface methodology (RSM) was used with the central composite design to evaluate and improve the drilling fluid compositions in terms of various rheological parameters.

Keywords: drilling fluid; rheology; filtration loss; diethanolamine; starch; thermal stability.

1. Introduction

Currently, energy sources are numerous, and crude oil remains one of the most valuable and dominant natural resources in the energy community [1]. According to reports of international energy organizations, the rate of oil demand is increasing steadily, due to the growing population and economic growth, especially in East Asian countries [2, 3]. Recently, 30-60% of the oil produced was obtained from wells that were recently discovered, due to the difficulty of discovering new reservoirs [4]. The drilling process is the drilling of a hole in the different layers of the earth to reach the formations those contain the petroleum crude according to the geological and exploration data [5]. In the drilling process, injected mud is one of the most common materials used in rotary drilling systems, and performs many tasks such as cooling the drill bit, cleaning the wellbore from crushed rock aggregates, preventing the escape of reservoir fluids, and stabilizing the wellbore [6].

Water drilling fluid is commonly used in formations as it is economically reasonable, and environmentally friendly. However, there are many difficulties in its use as a good drilling fluid, including poor lubricating properties, high filtration loss, and increased drilling time. Controlling the drilling fluid formulation is one of the most important

*Corresponding author e-mail: nabelnegm@hotmail.com.; (Nabel A. Negm).
Receive Date: 09 November 2020, Revise Date: 19 November 2020, Accept Date: 09 December 2020
DOI: 10.21608/EJCHEM.2020.49243.3010

matters for workers in the field of drilling fluids in controlling the filtration. Consequently, increasing the efficiency and ability of the drilling fluid to perform its functions in an economical manner is one of the priorities for research in this field, taking into consideration the environmental aspects. To avoid losing large amounts of drilling fluids during the process, several additives such as bentonite, carboxymethyl cellulose (CMC), and starch [7] are added to control the filtration losses. Bentonite has good properties such as fine particles, considerable surface area, good thermal stability, and high swelling ability in water. Recently, biodegradable poly-L-arginine was added to the drilling fluid to improve the stability of the wellbore. The addition of 2% poly-L-arginine to the drilling fluid [8] inhibited the swelling, and increased the stability of bentonite, and recovery to ~70% at 356 °F. The rheological behavior (shear-thinning) is one of the most important characteristic of drilling fluids, as it must be very viscous or even gel at zero or low shear rates to effectively suspend the cuttings from the wellbore. However, the viscosity should decrease at higher shear rates to ease the fluids injection into the wellbore. Therefore, the researchers focused on studying some inorganic nanomaterials, such as the oxides of copper, iron, aluminum, zinc, silica, carbon, and graphene [9-13]. Similarly, organic nanoparticles such as nanocellulose, modified nanocellulose, protein, chitin, xanthan gum, polyacrylamide derivatives were used as rheological modifiers for drilling fluids [14-16]. These modifiers enhanced the viscosity of bentonite-water based mud not only at rest or lower shear rates but also improve the shear-thinning behavior [14-17].

The starch must be processed into a plasticizer, as the semi-crystalline starch granules are converted into a homogeneous amorphous substance [18]. This transformation occurs as a result of the breakdown of the hydrogen bonds between the starch molecules with each other and the formation of new hydrogen bonds between the starch and the plasticizer molecules simultaneously [19]. Starch granular rupture can be obtained in the presence of a suitable plasticizer by applying the thermo-mechanical process [20]. The plasticizing starch process requires the addition of approximately 20-30% of plasticizer. Whereas starch is a very hydrophilic substance, and water content is depended on the storage conditions. The percentage of water attached to starch can be controlled by replacing with less volatile compounds, and thus will convert it from the granular phase to a homogeneous plastic phase at high temperatures.

There are limited studies on the treatment of starch with plasticizers to suit the conditions of drilling reservoir with high pressure and temperature; most of them were polymers such as glycols [21, 22]. Therefore, this study purposes to add the diethanolamine to the bentonite-starch mixture to decrease the filtration loss at high temperatures to suit the drilling of new wells. The chemical composition and physical stability will also be verified after adding the diethanolamine in proportions range of 20-80% to bentonite-starch mixture. In order to investigate the mechanism of enhancing thermal stability, the bentonite-starch-diethanolamine cake were investigated using X-ray diffraction, FTIR, Raman spectroscopy. The research also optimized the rheological behavior of drilling fluids under conditions of: temperature range 75-375 °C, starch concentration ranges between 200-1000 ppm, diethanolamine (DEA) concentration of 0-1000 ppm, and shear rate 5.1-1020 S^{-1}. To design the experiments, the CCD experimental process was optimized using response surface methodology (RSM).

2. Material and methods

2.1. Materials

Bentonite (BT) and starch were supplied from Sphenix Milling Station. Diethanolamine (DEA, HN $(CH_2CH_2OH)_2$, ≥98.5%) was purchased from Sigma Aldrich.

2.2. Mud formulation

Water-based fluid (WBF) samples were prepared (according to the API requirements) by adding bentonite (32 g, 6-wt%) to freshwater (500 mL) and starch (represents a ratio of 0.56% and 0.94% by weight of the amount of water and bentonite amount used) as standard experiments for the rheological properties and filtration loss control, and the samples were donated as: 0.56%-St-WBF and 0.94%-St-WBF. To study the Effect of diethanolamine, 0.19% to 0.75% (by weight), which represents 1-4 mL of the diethanolamine, and the samples were donated x%-y%-DEA-St-WBF, where x and y represented the weight percent of diethanolamine and starch, respectively. The mixtures were homogenized under stirring by Hamilton beach multi-mixer for 20 min, and the pH was adjusted at 10. The results of the

rheological tests were obtained at different temperatures (ambient, 300 °F, 320 °F, 350 °F, and 375 °F) using an oven controller.

2.3. Characterization

The diethanolamine, x%-St-WBF, y%-WBF, and x% St-y%-DEA-WBF skeletal chemical changes were monitored using Fourier transform spectroscopy recorded in the absorption mode. Samples were mixed with dried KBr, and the information was obtained at a rate of 32 scans with a resolution of 4 cm–1 from 400 to 4000 cm^{-1}. Raman spectroscopy of x%-St-WBF, y%-WBF, and x% St-y%-DEA-WBF samples was carried out by Bruker Raman instrument fitted with a diode Nd: YAG laser (λ = 532 nm). The X-ray diffraction patterns of the x%-St-WBF and x%-St-y%-DEA-WBF were recorded performed by Malvern Panalytical-X-Ray Diffractometer (XRD)-X'Pert Powder with Cu-Kα radiation. The monochromator was adjusted at a voltage (40 kV) and an intensity of 40 mA.

The drilling fluid was optimized using response surface methodology (RSM) provided by Design-Expert software 11.0 (Stat-Ease Inc., Minneapolis, USA). Central composite design (CCD) was applied to study the variables affecting the rheology of drilling fluids. Four independent variables identified are A: temperature (75-375 °F), B: starch concentration (200-100 ppm), C: DEA concentration (0-1000 ppm), and D: shear rate (5.1-1020 S^{-1}) and the response selected was AV, which was obtained from the rheometer. The ranges and levels of the five independent variables and responses with actual and coded levels of each parameter are listed in Table 1&2. There were two levels: low (−1) and high (+1), and the independent variables were coded to these two levels. In Table 3, real and coded independent variables are presented, and the results are given in the complete design matrix corresponding to the CCD design.

Table 1: Factor and response coded for the rheological parameters of drilling fluid

Factor	Name	Units	Min.	Max.	Coded Low	Coded High	Mean	Std. Dev.
A	Starch Concentration	ppm	200	1000	-1 ↔ 200.00	+1 ↔ 1000	56.67	26.82
B	DEA Concentration	ppm	0.00	1000	-1 ↔ 0.00	+1 ↔ 1000.00	51.33	32.67
C	Temperature	ºF	75	375	-1 ↔ 75.00	+1 ↔ 375.00	237.50	116.29
D	Shear rate	S^{-1}	5.1	1020	-1 ↔ 5.10	+1 ↔ 1020.00	511.19	387.59

Table 2: Response and response code for the rheological parameters of drilling

Response	Name	Units	Obs.tion	Min	Max	mean	Std Dev	Ratio
R1	AV	cP	30	8	32.5	17.9	7.24	4.06
R2	PV	cP	30	2	9	4.77	2.18	4.50
R3	YP	D/cm^2	30	10	51	24.77	9.70	5.10
R4	GL		30	2	24	9.77	6.63	12.00
R5	Thixo		30	1	6	2.57	1.48	6.00

Table 3: Experimental design matrix and experimental results of the response for rheological parameters

Run	A	B	C	D	AV, cP	PV, cP	Yield point, D/cm^2	GL	Thixo.
1	200	200	375	510	10	3	22	2	1
2	600	200	350	510	13	4	24	3	2
3	1000	600	75	340	29	5	44	18	5
4	400	600	75	510	26	4	37	15	4
5	600	1000	75	5.1	21	3	32	12	3
6	800	1000	225	1020	14	2	18	5	1
7	1000	200	300	1020	18	8	20	6	4
8	200	200	325	510	12	4	25	3	1
9	600	1000	225	1020	15	2	21	8	2
10	600	200	375	5.1	12	4	10	4	2
11	400	1000	225	5.1	17	3	26	10	2
12	1000	200	75	340	32.5	7	51	24	6
13	600	600	375	5.1	10	2	16	5	1
14	200	200	75	1020	27	7	31	18	4
15	400	200	375	5.1	9	6	10	3	1
16	200	0	375	1020	11	8	15	4	2
17	600	200	375	5.1	12	3	20	2	1
18	200	1000	225	1020	15	2	20	8	1
19	1000	400	225	1020	25	6	30	15	4
20	200	1000	225	5.1	15	4	24	9	2
21	800	600	300	510	14	4	19	6	2
22	600	600	75	510	28	8	32	20	5
23	600	800	225	510	16	2	24	8	1
24	400	400	225	510	17	3	25	9	2
25	600	400	375	1020	10	7	12	4	2
26	400	400	75	1020	28	8	33	20	4
27	400	200	375	510	8	5	10	3	1
28	600	1000	225	340	19	4	29	13	3
29	1000	400	225	340	24.5	6	29	14	4
30	800	600	75	170	29	9	34	22	4

A: Starch concentration (ppm); B: DEA concentration (ppm); C: Temperature (°F); and D: Shear rate S^{-1}

2.4. Mud testing

2.4.1. Rheological properties

According to requirements of the API code, apparent viscosity (AV, cP), plastic viscosity (PV, cP), yield point (YP, $Ib/100ft^2$), gel strength (GL, $Ib/100ft^2$), and thixotropy (Thixo, $Ib/100ft^2$) of all prepared samples were measured with a viscometer Chan 35 Model 3500 API Viscometer. The viscometers dial readings were recorded at different speeds, 600, 300, 200, 100, 6, and 3 rpm. Rheological properties of differently prepared samples were measured at ambient and different temperatures [23].

2.4.2. Filtration test

The ability of the prepared samples to reduce fluid loss was tested using a device (OFITE testing API Stander Filter press 6 cups). The test was performed by pouring the fluid into a stainless steel chamber with a bottom open. The mud is exposed to a pressure of 100 psi for 30 minutes, and the amount of filtered

water is recorded. Also, the thickness of the mud cake was determined on the filter paper by the low-pressure press.

3. Results and Discussion

3.1 Characterization of the prepared samples

FTIR spectra of DEA, bentonite, and starch were shown in **Figure 1a**, and FTIR of 0.93%St-WBF, 1%-DEA/St, 0.37%-DEA/bentonite, and 0.37%-DEA -0.94%-St-WBF were shown in **Figure 1b**. FTIR chart of the DEA shows peaks at 3380 cm^{-1} (O–H stretching), 2970 and 2888 cm^{-1} (–C–H symmetric and asymmetric stretching), 1587 cm^{-1} (N-H bending), 1492 (C–H scissoring), 1393 and (C–H bending), 1329 cm^{-1} (O-H bending), 1074 (–N–C stretching), and 1029 cm^{-1} (C-O stretching). FTIR of starch shows broad peaks at 3385 cm^{-1} (O–H stretching); the broadness indicates hydrogen bonding interaction between starch moieties or water molecules and starch moieties. The interaction of starch moieties and water molecules is characterized by the presence of a medium peak at 1642 cm^{-1} (O–H bending). The fingerprint peaks of starch can be seen in region 1200 to 950 cm^{-1} due to the presence of glycosidic rings (binding mode of –C–O–, –C–C– and –C–H–O groups) [14, 24]. FTIR of bentonite (BT) shows peaks at 3700 cm^{-1} (stretching Al–OH–Si), 3632 cm^{-1} (stretching Al–OH–Mg), 3428 (stretching –OH), 1640 cm^{-1} (bending –OH), 1040 cm^{-1} (stretching –Si–O–Si–), 917 cm^{-1} (stretching (Si–O–Al), 798 cm^{-1} (Al–OH–Mg), 695 cm^{-1} (binding Si–O–Al), and 470 cm^{-1} (rocking Al–Mg–OH) [25, 26]. By adding starch to bentonite (**Figure 1b**), the peak of hydroxyl groups appeared at 3437 cm^{-1}, which has lower energy than both bentonite and starch. This blue shift indicates the formation of hydrogen bonds between hydroxyl groups of bentonite and starch moieties. Moreover, adding DEA to the bentonite and starch mixture, the hydroxyl groups were appeared at 3419 cm^{-1}, which has higher energy than bentonite and starch, and lower than DEA.

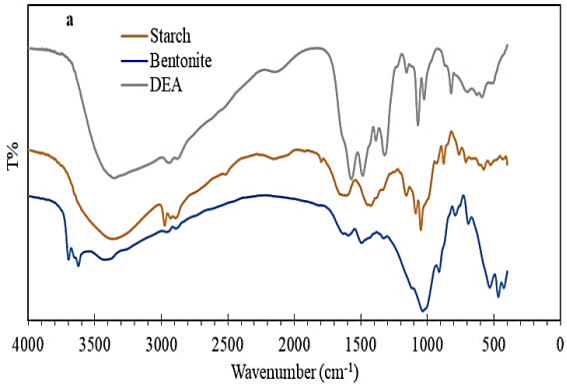

Figure 1a: FTIR spectra of DEA, bentonite, and starch.

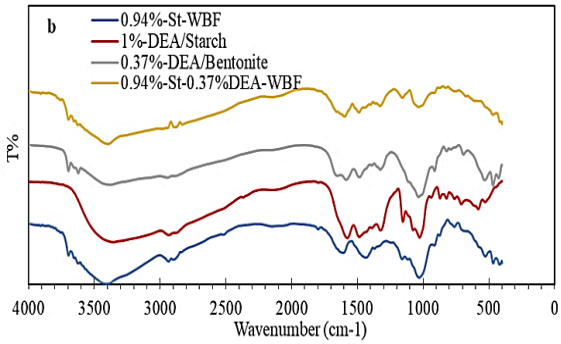

Figure 1b: FTIR of 0.93%St-WBF, 1%-DEA/St, 0.37%-DEA/bentonite, and 0.94%-St-0.37%DEA-WBF.

This behaviour may be indicated that DEA enables starch to glides between bentonite layers and restricted the vibrations of both the hydroxyl group of bentonite and starch. On the other hand, DEA may be protonated by the Bronsted acid group of bentonite (Al–OH–Si), leading to the disappearance of the hydroxyl group of bentonite, and therefore it can be concluded that this peak concerns only the amine and starch hydroxyl groups, which has lower energy than that of both. To confirm this behavior, FTIR of DEA and bentonite was done, where the hydroxyl group appeared at 3416 cm^{-1}, which is in between the hydroxyl group of bentonite and DEA. This change is associated with the formation of a new peak at 1330 cm^{-1} [27], implying the formation of onium salt (bis(2-hydroxyethyl) ammonium $(Al–O–Si)^{-}$). The hydroxyl groups of starch and diethanolamine mixture appeared at 3395 cm^{-1} with a blue shift of 5 cm^{-1} and 10 cm^{-1}, respectively, which can be attributed due to the formation of the hydrogen bonds.

Raman spectra of bentonite, 0.93%St-WBF, and 0.37%DEA-0.94%-St-WBF samples were shown in **Figure 2**. The Raman spectra of bentonite show the stretching and wagging vibration of the oxygen atom in silica framework at 448 cm^{-1} and 615 cm^{-1}, respectively. The peak at 899 cm^{-1} is attributed to the silica framework (–Si–O–Si-) [28]. The metal substituted silica framework like aluminium and magnesium peaks were also obtained. After the addition of starch and DEA, the intensities of 448 cm^{-1} and 615 cm^{-1} peaks were decreased and overlapped as a result of the interaction of surface groups with starch. The bentonite peak intensity at 1320 cm^{-1} was enhanced and shifted to lower value due to the insertion and intercalation of organic material (CH_2-twisting vibrational mode) [28] within

bentonite layers. Moreover, The interaction between the hydroxyl group of bentonite and water molecules (hydrogen bond) was appeared at 1610 cm^{-1} [29] with increased intensity after adding of starch and DEA, suggesting the strengthening of hydrogen bonds formation in the mixture.

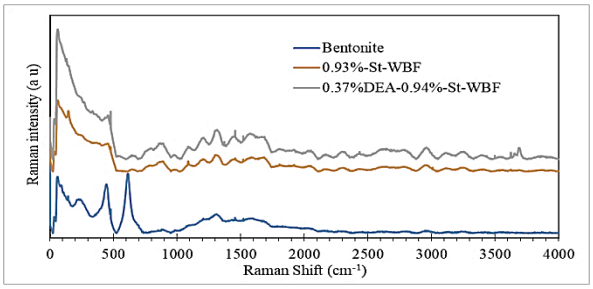

Figure 2: Raman spectra of bentonite, 0.93%St-WBF, and 0.37%DEA-0.94%-St-WBF samples.

XRD analyses of bentonite, 0.93%St-bentonite, 1%-DEA/Bentonite, and 0.94%-St-0.37%DEA-WBF were displayed in **Figure 3**. XRD of bentonite shows major peak at 8.9° (*d*=0.99 nm), 12.6°(*d*=0.7 nm), 19.8°(*d*= 0.45 nm), 20.4°(*d*=0.44 nm), 21°(*d*=0.42 nm), 25.02°(*d*=0.36 nm), 26.75°(*d*=0.33 nm), 31.78°(*d*=0.28 nm), 36.64°(*d*=0.25 nm), 45.6°(*d*=0.2 nm), 50.2°(*d*=0.18 nm), 60.16°(*d*=0.15 nm), and 68.24°(*d*=0.14 nm). After mixing bentonite and starch (0.93%St-bentonite), the peak at 8.9° was shifted to lower 2θ (7.28°, *d*=1.21), indicating the insertion of starch molecules between clay layers. Also, the other peaks showed a reduction in the intensity due to the separation of some layer, and consequently, the particle size of bentonite is reduced. Similar behavior was obtained in DEA-bentonite mixture (0.94%-St-0.37%DEA-WBF). The mixed form of bentonite, starch, and DEA showed XRD peak similar to bentonite clay, noting that the *d*-spacing between bentonite layers is greater than the pure clay. This behavior may result from the strong hydrogen bond interaction between starch and bentonite in the presence of DEA.

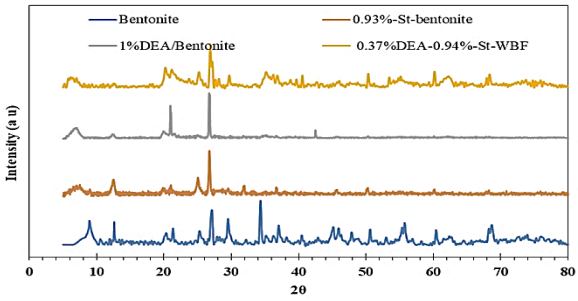

Figure 3: XRD patterns of bentonite, 0.93%St-bentonite, 1%-DEA/Bentonite, and 0.94%-St-0.37%DEA-WBF.

3.2. Rheological Properties of 0.56% and 0.93%St/WBF

The shear-stress shear-rate behavior of 0.56%-St/WBF and 0.93%-St/WBF at 350 °F is shown in **Figure 4a,b**. As shown in **Figure 4a**, all parameters, including AP (21 cP), PV (5 cP), YP (32 Ib/100ft^2), GL (8 Ib/100ft^2), and thixotropy (Thixo, 12) for WBF. Compared to bentonite free starch, 0.56%/WBF has a successful specification of drilling fluid within the API at 350 °F. With an increase in the amount of starch to 0.93%, an increase in the parameters was observed, as the sample was achieved AP (27.5 cP), YP (45 cP), Gel (15 Ib/100ft^2), and for 0.93%St/WBF, while PV (5), and Thixo (3) was achieved less values, however, these values are within the API (**Figure 4b**). Moreover, the 0.93%-St/WBF showed a behavior very closed to the rheological behavior of 0.56%-St/WBF; however, all rheological parameters are improved (**Figure 5a,b)**.

3.3. Effect of addition diethanolamine on the rheological properties of 0.56% and 0.93%St/WBF.

Figure 4a,b, and **Figure 5a,b** shows the Effect of the addition of DEA (0.19, 0.37, and 0.75%) on the rheological properties of WBF. From **Figure 4a**, shear stress increased with increasing shear rate and shows the effect of a given concentration of DEA at the presence of starch (0.56%) on shear stress at 350 °F. There is a similarity between blank (0.56%-St/WBF) and the three concentration additives to the WBF, in which there is an increment for the addition of DEA by 0.19% and 0.37% (**Figure 4b**).

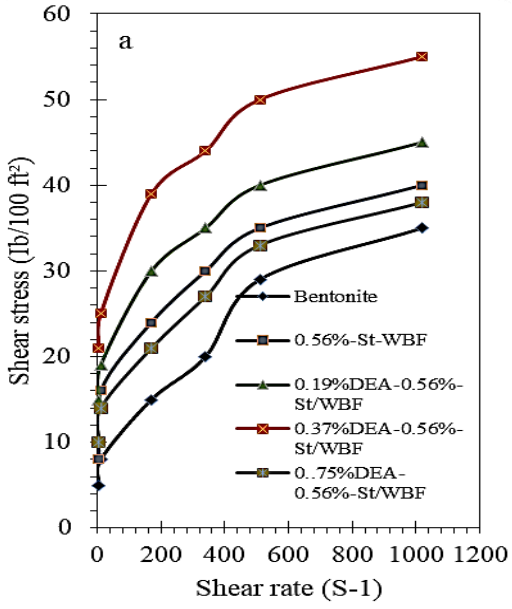

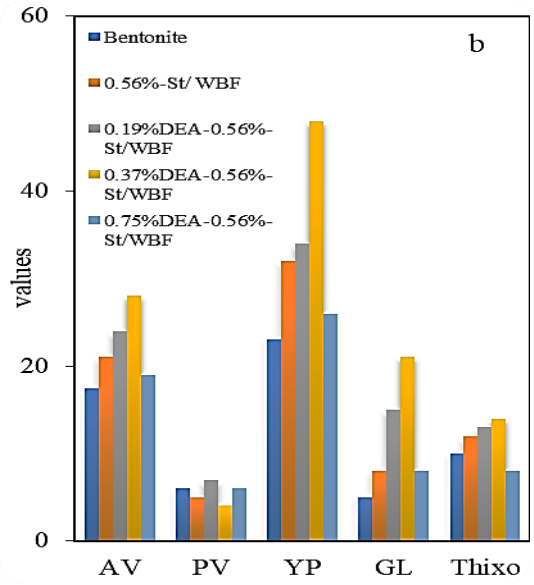

Figure 4: (a) Shear rate/shear stress of 0.65%St/WBF for different DEA concentrations at 350 °F; (b) rheology of mud at different DEA concentrations at 350 °F.

The increase of DEA to 0.75% led to a decrease in the rheological properties of WBF. The same behavior was observed for 0.93%-St/WBF (**Figure 5a,b**), considering that the values inferred from the shear rate-shear stress were enhanced by a clear sign, as these values achieved AP (30 cP), YP (50 cP), Gel (21 Ib/100ft^2), PV (5 cP), and Thixo (4 Ib/100ft^2) for 0.19%-DEA-0.93%-St/WBF. This values were reached AP (32 cP), YP (51 cP), Gel (24 Ib/100ft^2), PV (7 cP), and Thixo (4 Ib/100ft^2) for 0.37%-DEA-0.56%-St/WBF. However, 0.75%-DEA-0.93%-St/ WBF rheological values are some very closed to the data obtained from the blank sample (0.93% St/WBF).

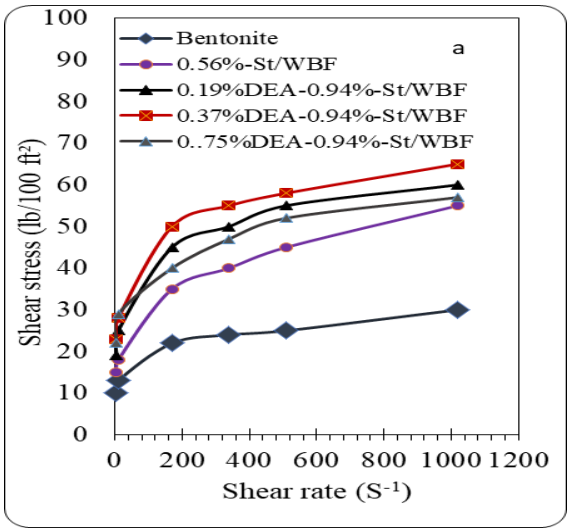

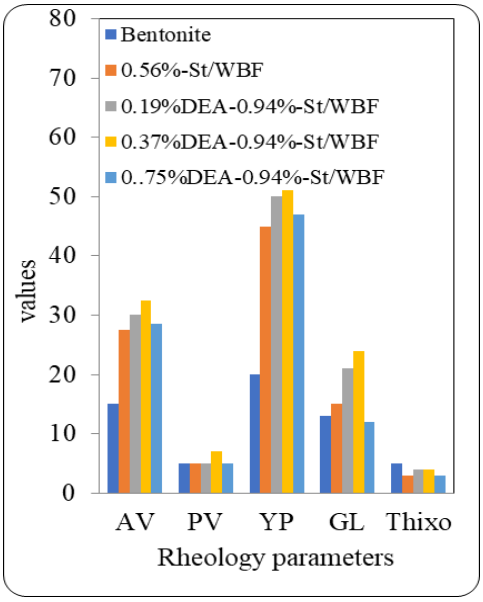

Figure 5: (a) Shear rate/shear stress of 0.94%-St/WBF for different DEA concentrations at 350 °F; (b) rheology of mud at different DEA concentrations at 350 °F.

3.4. Effect of temperature on the rheological properties of 0.19%DEA-0.93%St/WBF

Figure 6 shows the effect of temperature on the rheological of the WBF (0.19%DEA-0.93%St/WBF). It was evident that the addition of DEA to bentonite or starch-bentonite significantly improved the thermal stability of both samples. This behavior may be attributed to the binding of DEA to the Lewis acid site by forming a coordinated bond between the nitrogen atom of DEA and the Lewis acid site in bentonite, which results in increased swelling properties of the bentonite and thus improves the rheological properties of the bentonite. By adding DEA to starch-bentonite, DEA creates a hydrogen bond between the starch and bentonite through it, meaning that the DEA acts as a cross-linking agent, improving the thermal stability of the 0.19%-DEA-0.93%-St/WBF. This behavior has also been observed by others, who have found that DEA leads to an improvement in the rheological properties of the drilling fluid. However, the addition of DEA leads to more improvement in the rheological properties of the drilling fluid.

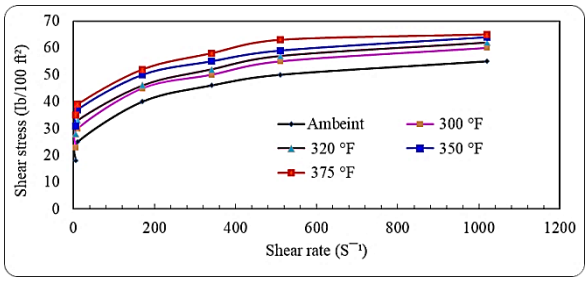

Figure 6: Effect the addition of 0.19%-DEA to 0.94%-St/WBF on the rheological properties of 0.19%DEA- 0.94%-St/WBF at deferent temperatures.

3.5. Effect of DEA addition on the filtration loss

Fluid loss or filtration is a measure of the flow of drilling fluids into the porous formation. Filtration is one of the most important characteristics of drilling fluids, as the drilling fluid creates a thin filter on the side of the well to decrease the loss of using the drilling mud to the formation. A good drilling fluid is one that maintains the concentrations of its components in a high proportion to control formation damage. **Figure 7a,b** shows the filtration loss and mud cake thickness of 0.56%-St/WBF with different concentrations of DEA. The WBF (0.94%-St/WBF) sample with a concentration of 0.19% and 0.37% DEA represents the lower filtrate volume is obtained with increasing the percentage of DEA. The filtration loss was 22 cm^3, 19 cm^3, 18 cm^3, and 14 cm^3 for 0.56%-St/WBF,0.19%-DEA-0.56%-St/WBF, 0.37%-DEA-0.65%-St/WBF, and 0.75%-DEA-0.56%-St/WBF, respectively.

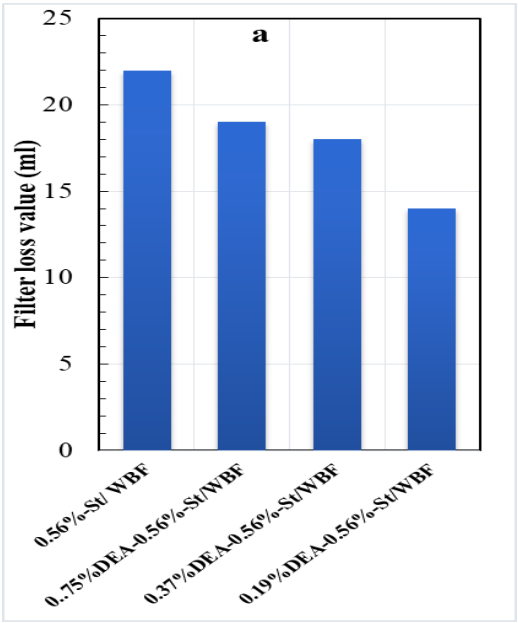

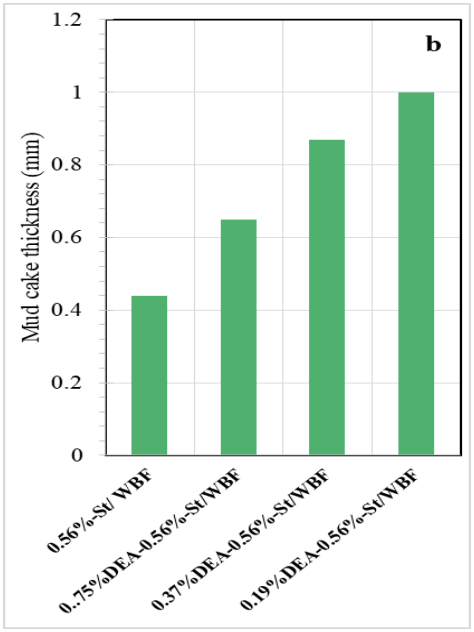

Figure 7: (a) the filtration loss amount; (b) mud cake thickness of mud fluid at different DEA-concentrations.

Moreover, **Figure 8a** shows a comparison between the rheology properties of 0.19%-DEA/bentonite and 0.19%-DEA-0.94%-St/WBF. It is clear that the rheological data obtained from DEA-bentonite and 0.19%-DEA-0.94%-St/WBF at high temperature (350 °F). The addition of DEA has a positive effect on all samples, where the basicity of DEA enabled its flow inside bentonite layers. This may increases the surface area of the bentonite, reflecting more layers in contact with water molecules. This interaction leads to increase the stability of bentonite-based drilling fluid. Moreover, the intercalated layer by DEA will be in contact with the starch molecule in solution, which increases the thermal stability of starch through the protection of starch moieties by the clay layers. Various researches reported that the bentonite layer acts as a thermal insulator of polymer, and were concluded that the thermal stability of the nanocomposite was more than the pure one [30-33]. A comparison between the filtration loss of 0.19%DEA-bentonite and 0.19%DEA-0.93%St/WBF is shown in Figure 9. The achieved data agree with the API; however, the modification of WBF using starch showed unique results at very low concentration of DEA (**Figure 8b**).

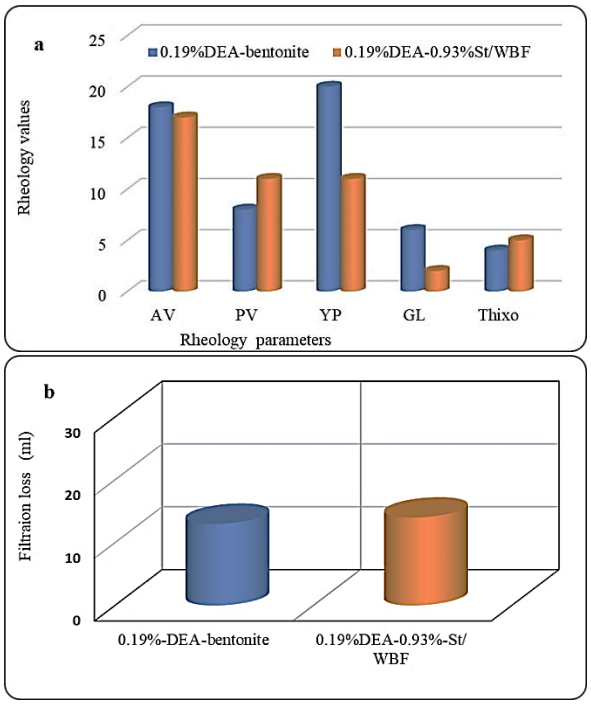

Figure 8: (a) Comparison between the rheology properties of 0.19%-DEA/bentonite and 0.19%-DEA-0.94%-St/WBF; (b) Comparison between the filtration loss of 0.19%-DEA/bentonite and 0.19%-DEA-0.94%-St/WBF.

Figure 9 represents the viscosity of the prepared drilling fluid and different percentages of DEA drilling fluid to the shear rate. All samples of the drilling fluid showed a significant viscosity at low shear rates relative to bentonite-based mud, and starch-bentonite-based mud, while the samples showed low viscosity values at high shear rates, which is known as shear thinning [34]. It also appears that the addition of DEA to starch-bentonite WBF increased the viscosity with a direct proportional to the additions of 0.19% and 0.37%. Further increase in DEA concentration showed a reduction in the obtained viscosity. This behavior has been observed by Bavoh et al. [35] using ammonium salt, and was attributed to the colloidal formation [35, 36].

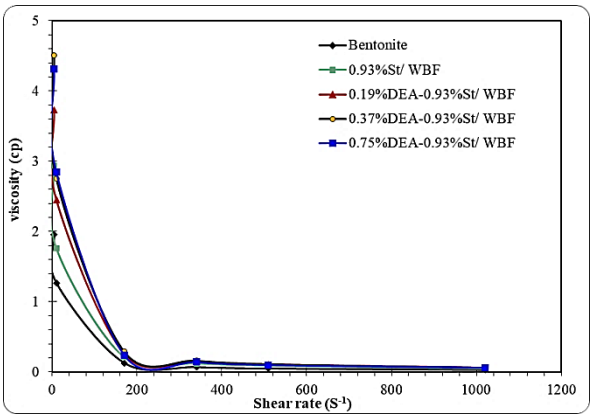

Figure 9: Viscosity vs. shear rate for the prepared samples.

3.6. Role of DEA on enhancing the rheological properties

The bentonite clay consists of several layers connected to each other through a strong van der Waal forces. These layers are negatively charged resemble plates like structure due to the imbalance between the valency of the silica and aluminium (major components) that constitute these plates. The bentonite has an isoelectric point (IEP) as their surface carries negative charges at the higher pH value and carries positive charges at a low pH. Because of the asymmetry between the valence of silicon atom and aluminium atoms, especially at edges Al−O^-, Al−OH_2, and Al−OH moieties in the basic, acidic and neutral solutions [16, 37]. Moreover, it has been reported that the attraction of negative charges on the surface of the bentonite plates and the positive charges at the edges of these plates are responsible for the bentonite viscosity through the attraction with water molecules [38]. DEA molecules are hydrophilic and weak base through the –NH– groups. The –NH– groups can be attacked by betonies' strong Lewis acid site, suggesting a more hydrophilic character of bentonite plates. The end-capped hydroxyl group of DEA can be hydrogen-bonded to the starch molecule, causing a more viscous solution or improvement of the rheological properties. The number of positively charged edges and corners is decreased by increasing the DEA percentage, as the solution's pH is turned somewhat higher. Consequently, the number of DEA bonded to the Lewis acid site decreases, and bentonite hydrophilicity decreases. From the obtained results, it can be assumed that the interaction between DEA modified bentonite plates is stronger than the interaction of bentonite and starch due to the DEA

increasing the number of sites on clay plates that can bind to starch through hydrogen bonds.

3.7. Statistical analysis

The experimental data obtained from CCD for the rheological models were analyzed with the RSM model. **Eq. 1** illustrated the variables obtained from AV, PV, YP, GL, and Thixo coded and actually, where Y denotes the expected response, and xi and xj represent the coded independent variables; β0, βj are the random error; and ij and j are constant coefficients

$$Y=\beta o+\Sigma k\ j=1\ \beta jxj+\Sigma\Sigma i<j\ \beta i\ jxixj+\Sigma kj=\beta j\ j\ x2\ j+\varepsilon \quad \textbf{(Eq. 1)}$$

Analysis of variance (ANOVA) for model regression of the rheological parameters of drilling fluid is tabulated in **Table 4**, where the Predicted R^2 of AV, YP, and GL are 0.8797, 0.6628, and 0.7628, respectively, with a reasonable agreement with the adjusted R^2 of 0.9479; 0.8098 and 0.9654, respectively, i.e., the difference is less than 0.2. The Predicted R^2 of thixo is 0.5847, not as close to the Adjusted R^2 of 0.8311, as one might normally expect; i.e., the difference is more than 0.2. This may indicate a large block effect or a possible problem with the model. A negative Predicted R^2 of PV implies that the overall mean may be a better predictor of the response than the current model. In some cases, a higher-order model may also predict better. Also, Adeq Precision measures the signal to noise ratio. A ratio greater than 4 is desirable. The ratio of 20.661, 5.130, 13.171, 15.948, and 12.593 for AV, PV, YP, GL, and Thixo, respectively, indicating an adequate signal.

Table 4: Analysis of variance (ANOVA) for model regression of the rheological parameters of drilling fluid

	AV	PV	YP	GL	Thixotropy
Std. Dev.	1.65	1.68	4.23	2.06	0.6076
Mean	17.90	4.77	24.77	9.77	2.57
C.V. %	9.23	35.15	17.08	21.07	23.67
R^2	0.9731	0.6935	0.9016	0.9501	0.9126
Adjusted R^2	0.9479	0.4074	0.8098	0.9036	0.8311
Predicted R^2	0.8797	-0.8181	0.6628	0.7828	0.5847
Adeq Precision	20.6612	5.1302	13.1708	15.9480	12.5934

The reasonable agreement exists between predicted and experimental values are shown in **Figure 10.** This figure developed that the data well-fitted with the model and gives a good estimate of the system's response in the range studied.

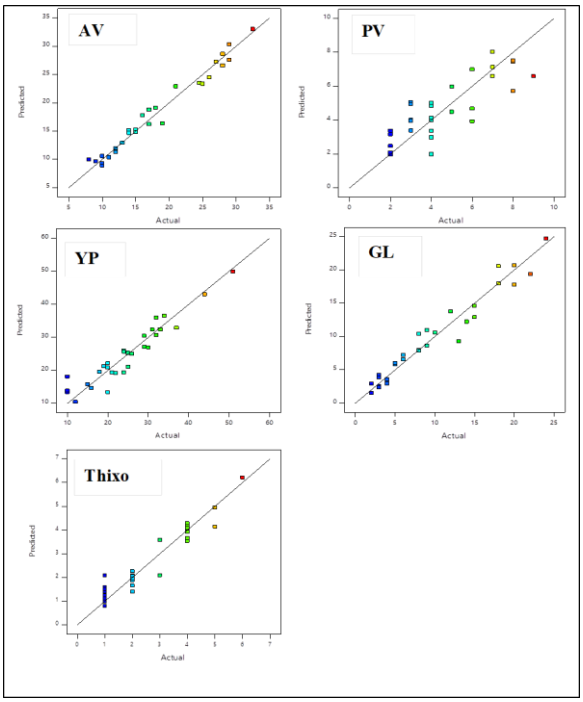

Figure 10: Predicted versus actual all rheological responses of the drilling fluid.

The model **Equations (2-11)** are based on the coded and actual values (A, B, C, and D as starch and DEA concentrations, temperature, and shear rate, respectively) for the AV, PV, YP, GL, and Thixo to study drilling fluid properties. From these figures, it was clear that the errors are insignificant, and the model is adequate and does not show any violation of the independence or constant variable assumption.

Coded AV=

$$19.82+2.70A-2.79B-8.79C+0.6193D-1.98AB-1.79AC-1.13AD-0.3467BC-1.77BD-.89CD-0.0162A^2-1.11B^2-1.50C^2+0.0785D^2 \quad \textbf{(Eq. 2)}$$

Actual AV=

$$12.77197+0.213940A+0.094376B+0.004425C+0.013352D-9.89x10^{-4}AB-2.98x10^{-4}AC-5.6x10^{-5}AD-4.6x10^{-5}BC-7.0x10^{-5}BD-2.5x10^{-5}CD-1.0x10^{-5}A^2-4.45x10^{-4}B^2-6.7x10^{-5}C^2+3.04667x10^{-7}D^2 \quad \textbf{(Eq. 3)}$$

Coded PV=

$$4.88+0.2419A-2.40B-1.35C+0.6426D-0.6556AB-0.8470AC+0.0678AD+0.2076BC-1.09BD+0.5241CD-0.8620A^2-0.7972B^2+0 \quad \textbf{(Eq. 4)}$$

Actual PV=

$$4.10589+0.117139A+0.019233B-0.006124C-0.003201D-0.000328AB-0.000141AC+3.33949x10^{-}$$

^{6}AD+2.8x10^{-5}BC-4.3x10^{-5}BD+6.88564E-06CD-5.39x10^{-4}A^{2}-3.19x10^{-4}B^{2} +1.49960x10^{-6}C^{2} +4.73968x10^{-6}D^{2}0337C^{2}+1.22D^{2}

(Eq. 5)

Coded YP=

26.02+2.71A-2.52B-10.16C+0.0498D-2.93AB-4.75AC-0.0219AD+2.73BC-2.67BD-2.12CD +1.20A^{2}+3.23B^{2}+0.7782C^{2}-4.73D^{2}

(Eq. 6)

Actual YP=

25.59787+0.229560A-0.119664B-0.039689C+ 0.030503D-0.001466AB-7.92x10^{-4}AC-1.07893x10^{-6}AD+3.64x10^{-4}BC-1.05x10^{-4}BD-2.8x10^{-5}CD +7.52x10^{-4}A^{2}+1.292x10^{-3}B^{2} +3.5x10^{-5}C^{2}-1.8x10^{-5}D^{2}

(Eq. 7)

Coded GL=

12.15+1.38A-1.96B-7.76C+0.7600D-2.38AB-4.27AC-1.45AD+2.37BC-2.54BD-1.80CD-2.30A^{2}-1.62B^{2}-1.20C^{2}+1.04D^{2}

(Eq. 8)

Actual GL=

-2.62398+0.462798A+0.077205B+0.011282C+ 0.011964D-1.190x10^{-3}AB-7.11x10^{-4}AC-7.1x10^{-5}AD+3.16x10^{-4}BC-1.0x10^{-4}BD-2.4x10^{-5}CD-1.435 x10^{-3}A^{2}-6.48x10^{-4}B^{2}-5.3x10^{-5}C^{2}+4.03786x10^{-6}D^{2}

(Eq. 9)

Coded Thixotropy=

2.43+0.9431A-0.8211B-1.36C+0.3435D-0.7723AB-0.1807AC+0.0134AD+0.0504BC-0.6501BD-0.2579CD+0.0284A^{2}+0.4105B^{2}+0.5076C^{2}-0.3119D^{2}

(Eq. 10)

Actual Thixotropy=

2.31705+0.047192A+1.95x10^{-3}B-0.016029C+3.923 x10^{-3}D-3.86x10^{-4}AB-3.0x10^{-5}AC+6.59013x10^{-7}AD+6.71541x10^{-6}BC-2.6x10^{-5}BD-3.38851x10^{-6}CD +1.8x10^{-5}A^{2}+1.64x10^{-4}B^{2} +2.3x10^{-5}C^{2}-1.2113x10^{-6}D^{2}

(Eq. 11)

3D plots for the interaction effect between previous independent variables toward the drilling fluid's response parameters are shown in **Figure 11&12**. These responses show a noticeable increase in all parameters with increasing DEA concentration up 200 ppm, then slightly increasing to 400 ppm. Above this concentration, the AV, PV GL, and thixo decreased due to hydrogen bonds forming between starch and DEA. On the other hand, the parameters decrease with increasing temperature for the blank sample. The addition of DEA improved the bond between starch and bentonite, leading to the samples' higher thermal stability.

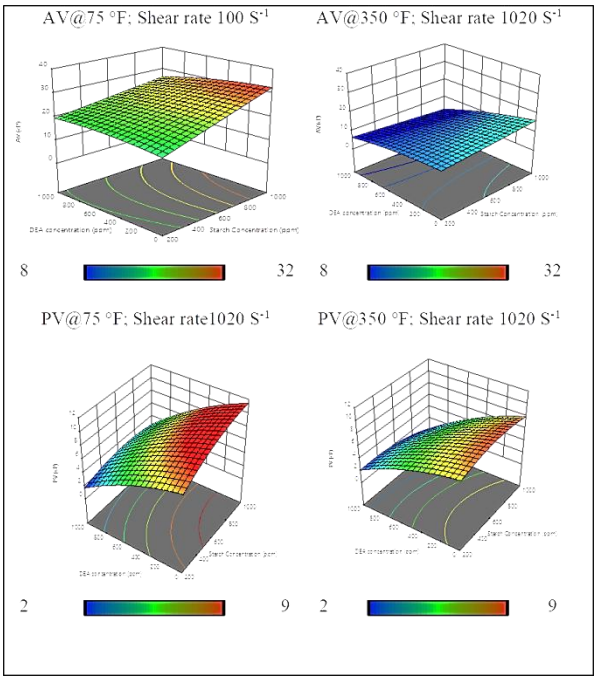

Figure 11: Effect of DEA and starch concentrations on AV and PV of the drilling fluid at different temperatures.

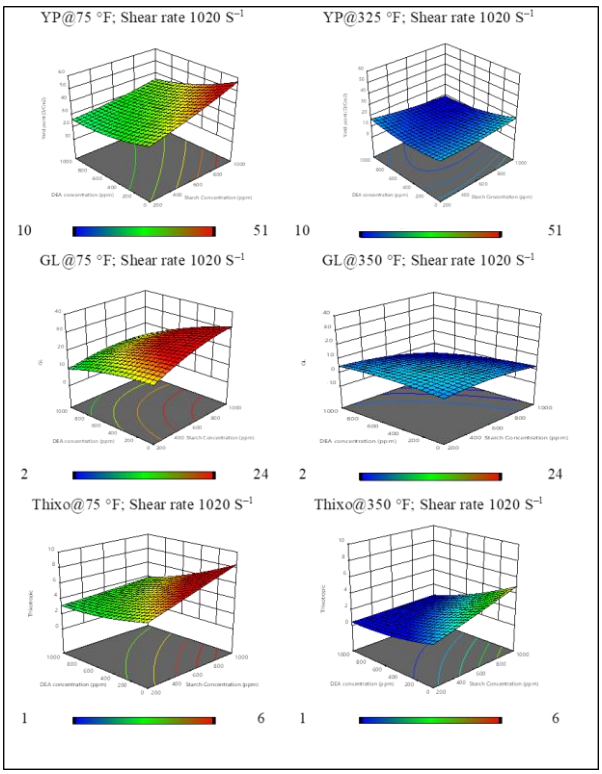

Figure 12: Effect of DEA and starch concentrations on YP, GL and Thixotropy of the drilling fluid at different temperatures.

3.8. Optimization

The range of the variables was set between low and high levels, coded as −1 and +1, to get the maximum

response for the drilling fluid rheology. The software generates a solution for these variables depending upon the model's desired response (**Figures 13**). The predicted values are 1000 ppm and 200 ppm for starch and DEA, respectively, that gives the high percentage rheological behavior and desirability value, 1.

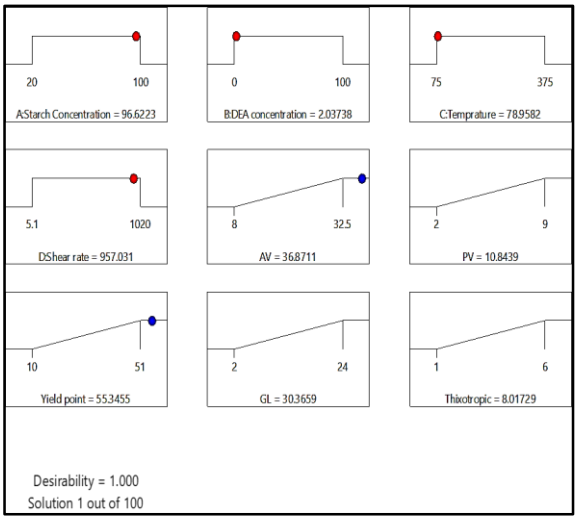

Figure 13: Contour optimization of all parameters for the rheological parameters of the formulated drilling fluid.

4. Conclusions

Diethanolamine was used to improve the rheological properties of water base mud formulating from bentonite and starch. The role of diethanolamine was comprised by bonding the starch and clay layers which increased the obtained thermal stability.

4. References

[1] D. Landa-Marban, F.A. Radu, J.M. Nordbotten, Transport in Porous Media 120 (2017) 395.
[2] J.A. Ali, K. Kolo, A. Khaksar Manshad, K.D. Stephen, Energy & Fuels 33 (2019) 927.
[3] J.A. Ali, K. Kolo, A.K. Manshad, K.D. Stephen, Journal of Molecular Liquids 284 (2019) 735.
[4] J.A. Ali, A.M. Kalhury, A.N. Sabir, R.N. Ahmed, N.H. Ali, A.D. Abdullah, Journal of Petroleum Science and Engineering 191 (2020) 107118.
[5] A. Fagan, Terminology 1 (1991).
[6] K. Van Dyke, Drilling fluids, mud pumps, and conditioning equipment. University of Texas at Austin Petroleum, 1998.
[7] P.L. Moore, (1986).
[8] X. Li, G. Jiang, X. Shen, G. Li, ACS Sustainable Chemistry & Engineering 8 (2020) 1899.
[9] M.M. Barry, Y. Jung, J.-K. Lee, T.X. Phuoc, M.K. Chyu, Journal of Petroleum Science and Engineering 127 (2015) 338.
[10] Z. Vryzas, L. Nalbandian, V.T. Zaspalis, V.C. Kelessidis, Journal of Petroleum Science and Engineering 173 (2019) 941.
[11] J.K.M. William, S. Ponmani, R. Samuel, R. Nagarajan, J.S. Sangwai, Journal of Petroleum Science and Engineering 117 (2014) 15.
[12] K. Wang, G. Jiang, F. Liu, L. Yang, X. Ni, J. Wang, Applied Clay Science 161 (2018) 427.
[13] A. Ismail, A. Aftab, Z. Ibupoto, N. Zolkifile, Journal of Petroleum Science and Engineering 139 (2016) 264.
[14] M.A. Betiha, G.G. Mohamed, N.A. Negm, M.F. Hussein, H.E. Ahmed, Arabian Journal of Chemistry 13 (2020) 6201.
[15] M.-C. Li, Q. Wu, K. Song, S. Lee, C. Jin, S. Ren, T. Lei, ACS applied materials & interfaces 7 (2015) 24799.
[16] M.-C. Li, Q. Wu, K. Song, Y. Qing, Y. Wu, ACS applied materials & interfaces 7 (2015) 5006.
[17] M.-C. Li, Q. Wu, K. Song, A.D. French, C. Mei, T. Lei, ACS Sustainable Chemistry & Engineering 6 (2018) 3783.
[18] J.J.G. Van Soest, D. De Wit, J.F.G. Vliegenthart, Journal of Applied Polymer Science 61 (1996) 1927.
[19] P. Jiping, W. Shujun, Y. Jinglin, L. Hongyan, Y. Jiugao, G. Wenyuan, Food chemistry 105 (2007) 989.
[20] H. Schmitt, K. Prashantha, J. Soulestin, M.F. Lacrampe, P. Krawczak, Carbohydrate Polymers 89 (2012) 920.
[21] K. Minaev, D. Martynova, A. Knyazev, A. Zaharov, I. Shenderova, IOP Conference Series: Earth and Environmental Science 21 (2014) 012035.
[22] M. Zoveidavianpoor, A. Samsuri, Journal of Natural Gas Science and Engineering 34 (2016) 832.
[23] V. Kelessidis, A. Mihalakis, C. Tsamantaki, 2005.
[24] C. Du, F. Jiang, W. Jiang, W. Ge, S.-k. Du, International Journal of Biological Macromolecules 164 (2020) 1785.
[25] M. El Bouraie, A.A. Masoud, Applied Clay Science 140 (2017) 157.

[26] F.G. Alabarse, R.V. Conceição, N.M. Balzaretti, F. Schenato, A.M. Xavier, Applied Clay Science 51 (2011) 202.
[27] M.E. Ramos, F.J. Huertas, Applied Clay Science 80-81 (2013) 10.
[28] F.L. Galeener, A.E. Geissberger, Physical Review B 27 (1983) 6199.
[29] H. Kaplan Can, Ö. Şahin, Journal of Macromolecular Science, Part A 52 (2015) 465.
[30] A. Usuki, N. Hasegawa, M. Kato, S. Kobayashi, in: F. Guida-Pietrasanta, B. Boutevin, O. Nuyken, O. Becker, G.P. Simon, K. Dusek, A.L. Rusanov, D. Likhatchev, P.V. Kostoglodov, K. Müllen, M. Klapper, M. Schmidt, A. Usuki, N. Hasegawa, M. Kato, S. Kobayashi (Eds.), Inorganic Polymeric Nanocomposites and Membranes, Springer Berlin Heidelberg, Berlin, Heidelberg, 2005, p. 135-195.
[31] B. Chen, J.R.G. Evans, H.C. Greenwell, P. Boulet, P.V. Coveney, A.A. Bowden, A. Whiting, Chemical Society Reviews 37 (2008) 568.
[32] M.S. Saharudin, S. Hasbi, MNA Nazri, F. Inam, in: S.S. Emamian, M. Awang, F. Yusof (Eds.), Advances in Manufacturing Engineering, Springer Singapore, Singapore, 2020, p. 107-129.
[33] H. Tan, L. Wang, X. Wen, L. Deng, E. Mijowska, T. Tang, Applied Clay Science 194 (2020) 105708.
[34] J. Plank, G. Keilhofer, P. Lange, Oil & gas journal 98 (2000) 39.
[35] C.B. Bavoh, Y.B. Md Yuha, W.H. Tay, T.N. Ofei, B. Lal, H. Mukhtar, Journal of Petroleum Science and Engineering 183 (2019) 106468.
[36] M. Naderi, E. Khamehchi, Journal of Petroleum Science and Engineering 163 (2018) 58.
[37] P.F. Luckham, S. Rossi, Advances in colloid and interface science 82 (1999) 43.
[38] G. Lagaly, Applied Clay Science 4 (1989) 105.